Homoepitaxial growth mechanism of ZnO(0001): Molecular-dynamics simulations

Momoji Kubo, Yasunori Oumi, Hiromitsu Takaba, Abhijit Chatterjee, and Akira Miyamoto*
Department of Materials Chemistry, Graduate School of Engineering, Tohoku University, Aoba-yama 07, Sendai 980-8579, Japan

Masashi Kawasaki
Department of Innovative and Engineering Materials, Tokyo Institute of Technology, Midori-ku, Yokohama 226-8503, Japan

Mamoru Yoshimoto
Materials and Structures Laboratory, Tokyo Institute of Technology, Midori-ku, Yokohama 226-8503, Japan

Hideomi Koinuma
CREST-JST and Materials and Structures Laboratory, Tokyo Institute of Technology, Midori-ku, Yokohama 226-8503, Japan
(Received 28 July 1998; revised manuscript received 28 February 2000)

We clarified here an epitaxial growth mechanism of ZnO(0001) surface on an atomic scale, by using molecular-dynamics crystal-growth simulations. It was observed that the crystal growth starts at the step of ZnO(0001), but not at the terrace of ZnO(0001). This phenomenon is clearly justified from the coordination number of adsorbed ZnO molecules on the ZnO(0001) surface. The ZnO molecule can form bonds with the smooth ZnO surface through only single coordination since the topmost surface is constructed by only one atomic species, i.e., either a Zn or O atomic plane. Hence, a ZnO molecule adsorbed on the smooth ZnO surface can be readily evaporated, indicating the rare growth of the ZnO(0001) from the terrace. On the other hand, double coordination can be observed at the step, since both Zn and O atoms are exposed to the surface at the step. Hence, the adsorbed ZnO molecule at the step is stabilized and the crystal growth starts from the step. It indicates that the ZnO molecule adsorbed at the step has a role of nucleation center. The above epitaxial growth mechanism is completely different from that of MgO(001) [M. Kubo *et al.*, J. Chem. Phys. **107**, 4416 (1997)]. This difference is clearly interpreted from the different surface structures of the ZnO(0001) and MgO(001).

I. INTRODUCTION

Artificial construction of atomically defined metal oxide layers is important in making electronic devices including light-emitting materials, high-temperature superconducting oxide films, magnetic devices, as well as other advanced materials.[1–6] Hence, the atomistic understanding of the epitaxial growth process of metal oxide surfaces is required to fabricate atomically controlled structure that exhibits unexplored and interesting physical properties.

On the other hand, wide and direct band-gap semiconductors have attracted much attention, due to their possible applications in blue light-emitting and ultraviolet laser-emitting devices. Initially a lot of efforts were concentrated on ZnSe,[7,8] but more recently GaN-based technologies have made a considerable advance.[9,10] However, their large threshold current and short lifetime are still the central issue of research and development. ZnO, an oxide semiconductor with a room temperature (RT) band-gap energy of 3.37 eV, is potentially another efficient RT ultraviolet emitter. It has a large exciton binding energy (60 meV) compared with those of GaN (28 meV) and ZnSe (19 meV), which should favor efficient excitonic emission processes at RT. Recently Kawasaki *et al.* constructed ZnO quantum dots on an α-Al_2O_3(0001) surface by using laser molecular-beam epitaxy techniques and observed an ultraviolet laser emission of the above material as pumped by a yttrium aluminum garnet (YAG) laser at RT.[11–13] After their reports, the studies on ZnO-based ultraviolet laser-emitting materials are rapidly stimulated.[14–19] Especially, the optical properties of the ZnO quantum dots were very sensitive to their crystal quality, orientation, and the size. Hence, in order to control these factors it is crucially important to understand the epitaxial growth mechanism of ZnO quantum dots on an atomic scale. Although important information on the epitaxial growth process of ZnO quantum dots has been obtained from a lot of experiments, theoretical approaches are also desired for the atomistic understanding of the epitaxial growth of ZnO quantum dots and for the artificial construction of efficient and long-lived ZnO-based ultraviolet laser-emitting materials. Although some crystal-growth molecular-dynamics (MD) simulations have been performed for Si films[20–24] and other systems,[25–29] there are no simulation studies devoted to the epitaxial growth process of metal oxide surfaces except our earlier works on the epitaxial growth of MgO(001) (Refs. 30 and 31) and $SrTiO_3$(001) (Refs. 32–34) surfaces. Hence, in the present paper we applied our crystal-growth MD simulation code MOMODY to investigate the homoepitaxial growth process of the ZnO(0001) surface. Especially, the effect of surface step on the crystal-growth process along with the atomistic mechanism of the epitaxial growth process were discussed.

II. METHOD

We employed our crystal-growth MD simulation code MOMODY, Version 2.0 in the present paper. The methodology of the crystal-growth MD is slightly different from regular MD simulations. The total number of species in the system is not fixed but increases with time. Figure 1 shows the model

system of these MD simulations: the top corresponds to the source of emitting metal oxide molecules and the substrate lies at the bottom. ZnO molecules, which emerge randomly from any point of the emitting source of metal oxide molecules, are emitted one by one at regular time intervals of 2 ps with a constant velocity of 900 m/s. We employed the same condition as our previous works on the homoepitaxial growth of the MgO(001) surface[30] for the direct comparison. Here, the vibration and rotation of the depositing ZnO molecules are considered.

Hence, by following the above procedure, the crystal-growth process of ZnO thin films can be simulated on an atomic scale. The Verlet algorithm was used for the calculation of atomic motions, while the Ewald method was applied for the calculation of electrostatic interactions. Temperature was controlled by means of scaling the atom velocities. Only the temperature of the bottom layer of the ZnO(0001) surface was controlled such that the energy released from the ZnO molecules is correctly reproduced from the deposition event. The calculations were performed for 30 ps with a time step of 2.0×10^{-15} seconds, and a total of 10 ZnO molecules were deposited on the ZnO(0001) surface. A slab model was used under the three-dimensional periodic boundary condition. The surface area and substrate thickness are 16.265 $\times$16.902, and 15.639 Å, respectively. The distance between the ZnO(0001) surface and the emitting source of metal oxide molecules is 20.852 Å and the thickness of vacuum phase is 46.917 Å. The system was equilibrated for 40 ps, prior to the epitaxial growth simulations.

The interatomic potential functions consist of two-body and three-body terms.[35,36] The two-body, central force, interatomic potential is described as follows for any atom pairs. In Eq. (1), the first, second, and third terms refer to Coulomb, exchange repulsion, and Morse interactions, respectively.

$$\begin{aligned} u(r_{ij}) = {} & Z_i Z_j e^2/r_{ij} + f_o(b_i+b_j) \\ & \times \exp[(a_i+a_j-r_{ij})/(b_i+b_j)] \\ & + D_{ij}[\exp\{-2\beta_{ij}(r_{ij}-r_{ij}^*)\} \\ & - 2\exp\{-\beta_{ij}(r_{ij}-r_{ij}^*)\}], \end{aligned} \tag{1}$$

where Z_i is the atomic charge, e the elementary electric charge, r_{ij} the interatomic distance, and f_0 a constant for unit adaptations. The parameters a and b represent the size and stiffness, respectively, in the exchange repulsion interaction, while D_{ij}, r_{ij}^*, and β_{ij} represent bond energy, equilibrium bond distance, and stiffness, respectively, in the Morse function.

The three-body potential, as shown in Eq. (2), is applied for Zn-O-Zn and O-Zn-O angles:

$$u(\theta_{ijk}) = -f_k[\cos\{2(\theta_{ijk}-\theta_0)\}-1]\times(k_1k_2)^{1/2}, \tag{2}$$

where θ_{ijk} is the angle between atoms $i-j-k$, and f_k and θ_0 are the parameters. The variables k_1 and k_2 define the effective range of the three-body potential:

$$k_1 = 1/[\exp\{g_{r1}(r_{ij}-r_{m1})\}+1], \tag{3}$$

$$k_2 = 1/[\exp\{g_{r2}(r_{jk}-r_{m2})\}+1], \tag{4}$$

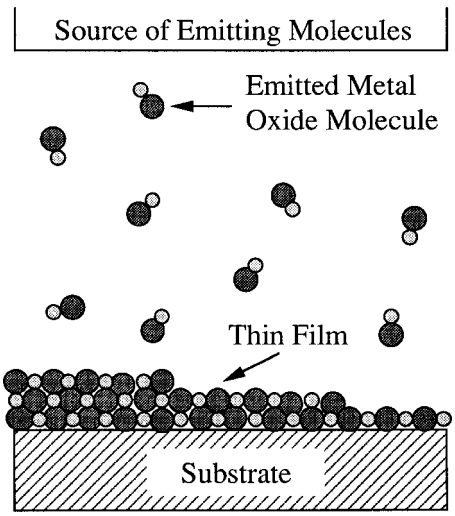

FIG. 1. Model system for simulating the epitaxial growth process of metal oxide surfaces.

where g_{r1}, g_{r2}, r_{m1}, and r_{m2} are the parameters. r_{ij} and r_{jk} are the interatomic $i-j$ and $j-k$ distances, respectively. The values of k_1 and k_2 are close to unity at the intramolecular Zn-O distance and approach to zero with the increment of the distance.

Calculations were performed on a Silicon Graphics Origin200 computer server, while the computer graphics (CG) visualization was made with an Insight II software[37] of Molecular Simulations Inc. on a Silicon Graphics Indigo2 workstation. Moreover, dynamic features in the epitaxial growth process were investigated by using real time visualization with the MOMOVIE code and RYUGA (Ref. 38) code developed in our laboratory and implemented on OMRON LUNA-88K workstation and Hewlett Packard Apollo 9000 Model 715/33 workstation, respectively.

III. RESULTS AND DISCUSSION

A. Development of force field for ZnO

The accurate force field for ZnO is required for the present purpose. The potential parameters for ZnO in Eqs. (1)–(4) were determined by using MD simulations, so as to reproduce the lattice constants and the expansion coefficients of ZnO crystal. The determined potential parameters of Zn and O atoms are presented in Table I. The calculated lattice constants and expansion coefficients of ZnO crystal, shown in Table II, are in good agreement with the experimental results.[39,40] The trajectories of Zn and O atoms in the ZnO crystal were also close to the average positions of atoms determined by the x-ray diffraction (XRD) technique.[39] Moreover, the mean-square displacements (MSD) of Zn and O atoms from the positions derived by the XRD were 0.003 and 0.003 Å^2, respectively. These MSD values are not significant in comparison to the temperature factor in the XRD analysis.

The normal low-pressure phase of ZnO is a hexagonal wurtzite structure, similar to the other group II-VI and group III-V semiconductors with first-row anions (BeO, AlN, GaN, and InN),[41] though metastable thin films of ZnO with the cubic zinc-blende structure have been reported.[42] Hence, the

TABLE I. Potential parameters of Zn and O atoms. (a) Two-body terms.

Atom	Z_i	a_i/Å	b_i/Å
O	−1.2	1.650	0.110
Zn	+1.2	1.211	0.100

Atom Pairs	D_{ij}/kcal mol^{-1}	β_{ij}/Å^{-1}	r_{ij}^*/Å
O-Zn	24.0	2.00	1.95

(b) Three-body terms

three body	$f_k/10^{-19}$ J	θ_0/degree	r_0/Å	g_r/Å^{-1}
O-Zn-O	7.0	109.5	2.20	10.0
Zn-O-Zn	4.0	109.5	2.20	10.0

total energies of ZnO crystals with wurtzite and zinc-blende structures calculated by the above potential parameters were compared, in order to check how well the above potential parameters describe the phase stability of ZnO crystals. The calculated total energies of the wurtzite and zinc-blende structures were 449.9 and 448.4 kcal/mol, respectively. It indicates that the wurtzite structure is more stable than the zinc-blende structure, which is in good agreement with the experimental observation[41,42] and the previous periodic Hartree-Fock calculations.[43]

In order to check how well the above potential parameters describe the surface properties of ZnO crystal in addition to the bulk properties, we investigated the surface energies of some ZnO surfaces. It is experimentally well known that the $(10\bar{1}0)$ and $(11\bar{2}0)$ are cleavage surfaces of ZnO crystal with wurtzite structure and the stability of both surfaces was previously well investigated.[44–47] Hence, we calculated the surface energies of the $(10\bar{1}0)$ and $(11\bar{2}0)$ surfaces of wurtzite type ZnO crystal and investigated their relative stability. The surface energies of the $(10\bar{1}0)$ and $(11\bar{2}0)$ surfaces obtained by the above potential parameters were 2.1 and 2.2 J/m^2, respectively. It indicates that the $(10\bar{1}0)$ surface is more stable compared to the $(11\bar{2}0)$ surface, which is in good agreement with the previous molecular mechanics results[47] based on the shell model by Nyberg *et al.*

In order to check how well the above potential parameters describe the bond creation and bond dissociation, the cohesive energies of some ZnO molecules were calculated and these values were compared with the density functional theory (DFT) calculation results. DMOL software package[48] of Molecular Simulations Inc. was employed for the DFT calculations. A Vosko-Wilk-Nusair functional[49] was used for the correlation energy terms in the total-energy expression. All DFT calculations were carried out with a double numerical basis set with polarization functions.[50] We employed ZnO, Zn_2O_2, Zn_3O_3, and Zn_4O_4 clusters for the calculation of the cohesive energies. The cohesive energy values of two, three, and four ZnO molecules calculated by the above potential parameters were 119.6, 259.8, and 352.5 kcal/mol, respectively. These values were in good agreement with the DFT values of 113.8, 267.6, and 334.1 kcal/mol for two, three, and four ZnO molecules, respectively.

The determined potential parameters for ZnO reproduced various properties of ZnO and therefore can be used for the simulation of the epitaxial growth processes.

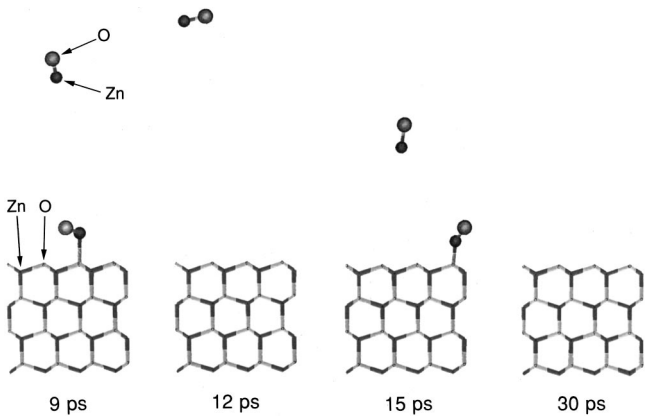

FIG. 2. Homoepitaxial growth process of smooth ZnO(0001) surface at 700 K.

B. Homoepitaxial growth process of smooth ZnO(0001)

Since ZnO crystal has a wurtzite structure, two different surface terminations by either Zn or O atomic plane at the (0001) surface are possible. Kawasaki *et al.* clarified that ZnO quantum dots on a α-$Al_2O_3(0001)$ surface is terminated by an O atomic plane by using coaxial impact collision ion scattering spectroscopy measurements,[14] and hence we employed a ZnO(0001) surface model terminated by an O atomic plane to be compared with experiments. Since Kawasaki *et al.* constructed ZnO quantum dots on a α-$Al_2O_3(0001)$ surface at 773 K,[11–13] we employed the sub-

TABLE II. Lattice constants and expansion coefficients of ZnO crystal derived from the MD simulations.

	a axis	*b* axis	*c* axis
Lattice constant [experimental result (Ref. 39)]	3.253 Å	3.253 Å	5.213 Å
Lattice constant (MD simulation)	3.246±0.002 Å	3.246±0.002 Å	5.232±0.002 Å
Expansion coefficient [experimental result (Ref. 40)]	5.50×10^{-6}/K	5.50×10^{-6}/K	5.00×10^{-6}/K
Expansion coefficient (MD simulation)	5.49×10^{-6}/K	5.47×10^{-6}/K	5.05×10^{-6}/K

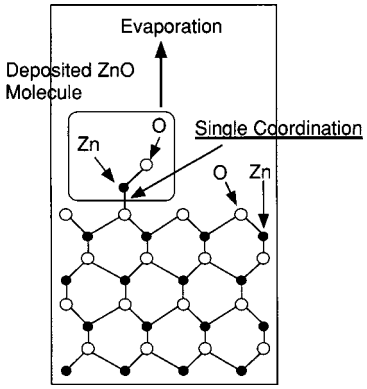

FIG. 3. Schematic position of the first adsorbed ZnO molecule on the smooth ZnO (0001) surface.

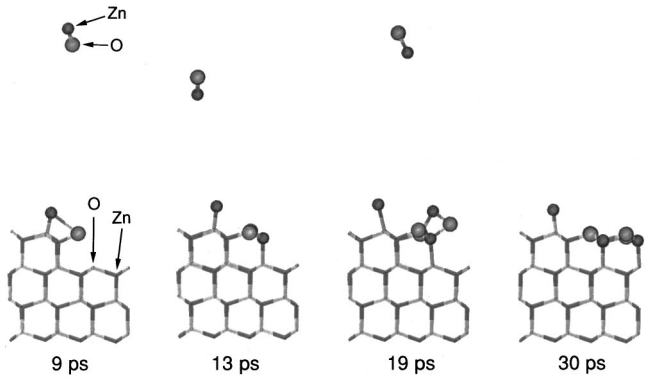

FIG. 4. Homoepitaxial growth process of the ZnO(0001) surface with a step at 700 K.

strate temperature of 700 K to be compared with experiments. Figure 2 shows the homoepitaxial growth process on the smooth ZnO(0001) surface terminated by the O atomic plane at 700 K. The ZnO substrate is shown by atomic bonds, while the deposited ZnO molecules are shown by both spheres and atomic bonds. One ZnO molecule stuck on the ZnO(0001) surface at 9 ps. The Zn atom of the deposited ZnO molecule is bonded to an O atom of the surface, indicating that the adsorbed ZnO molecule can form bonds with the surface through only single coordination. It is due to the fact that the topmost surface consists of only O atomic species and Zn atoms are not exposed at the surface. However, the adsorbed ZnO molecule was readily evaporated from the surface at 12 ps. We suggest that the small interaction resulting from single coordination favors the release of the adsorbed ZnO molecule from the surface at a high temperature of 700 K (Fig. 3). Although another ZnO molecule stuck to the surface again at 15 ps, it was also readily evaporated from the surface. Similar processes were repeated on the surface, and hence finally no ZnO molecule adhered to the smooth ZnO(0001) surface at 30 ps. It indicates that ZnO thin films or quantum dots rarely grow from the smooth ZnO(0001) surface.

C. Homoepitaxial growth process of ZnO(0001) with step

Experimentally, the ZnO(0001) surface is not completely smooth, and a lot of steps, kinks, and defects exist on the surface. Therefore, the understanding of the effect of the surface steps on the homoepitaxial growth process is essential to control the structures of ZnO thin films or quantum dots on an atomic scale. Hence, we simulated the continuous deposition process of ZnO molecules on a ZnO(0001) surface with a step. The surface terminated by O atomic plane is also employed for the present purpose. Figure 4 shows the results at 700 K. Surprisingly, the ZnO epitaxial film was smoothly constructed at 30 ps in contrast to the process on the smooth ZnO(0001) surface. It indicates that the crystal growth readily starts at the surface step, which is not realized at the smooth surface. Moreover, the deposited ZnO molecule kept a wurtzite structure and (0001) oriented configuration on the surface. The detailed mechanism of the above process is discussed below.

First, one ZnO molecule stuck to the step at 9 ps. Here, the Zn atom of the deposited ZnO molecule is bonded to an O atom of the surface, while the O atom of the deposited ZnO molecule is bonded to a Zn atom of the surface. Namely, the deposited ZnO molecule forms bonds to the surface through double coordination, which is much different from the process on the smooth ZnO(0001) surface. It is due to the fact that both Zn and O atoms are exposed at the step, which is not realized at the smooth surface. A second deposited ZnO molecule adhered to the step at 13 ps and a six-membered ring was formed at the step. This result indicates that the first adsorbed ZnO molecule at the step plays a role of the nucleation center. At 19 ps, one ZnO molecule stuck to the new step that was formed at 13 ps. Here, the adsorption structure of the single ZnO molecule at 19 ps is similar to that at 9 ps. After 19 ps, the next single ZnO molecule adsorbed at the new step and a new six-membered ring was formed, which was a completely similar process observed from 9 to 13 ps in Fig. 4. It indicates that the adsorbed ZnO molecule at 19 ps also plays a role of the nucleation center.

The similar processes repeated many times and finally the first ZnO layer was completely constructed at 30 ps. The detailed mechanism is summarized in Fig. 5. We should note that the deposited second ZnO molecule formed three six-membered rings at the same time, which greatly stabilized the second deposited ZnO molecule [Fig. 5(b)]. It may also be another reason, justifying that the epitaxial growth smoothly starts from the surface step. Experimentally, Ohtomo *et al.* revealed[15] that ZnO quantum dots are formed in a spiral growth mode on a α-Al_2O_3(0001) surface. Since

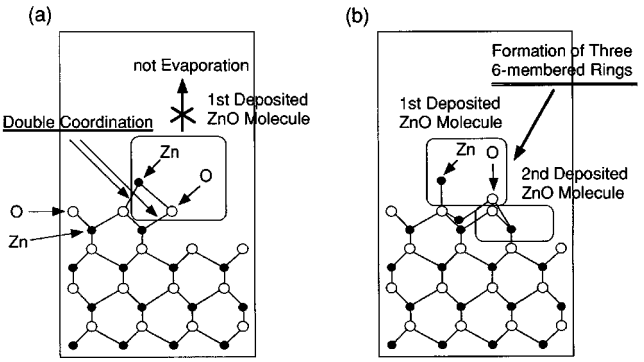

FIG. 5. Schematic position of the (a) first and (b) second deposited ZnO molecules on the ZnO(0001) surface with a step.

a spiral growth is realized by the step flow growth with screw dislocation, our MD simulation results support their experiments.

In order to confirm our results, we also performed 20 more calculations on the homoepitaxial growth process of both smooth and stepped ZnO(0001) surfaces. However, almost similar results were obtained as mentioned above. Hence, we confirmed the above crystal-growth simulation results.

D. Comparison with homoepitaxial growth process of MgO(001)

The above homoepitaxial growth mechanism is completely different from that of the MgO(001) surface.[30,31] MgO thin film grows epitaxially on a smooth MgO(001) surface, keeping NaCl type structure and (001) oriented configuration during the MD simulation. Moreover, surface steps do not greatly affect the growth process of the MgO(001) surface. This difference is clearly interpreted from the surface structure of the MgO(001) surface. Since MgO crystal has a NaCl type structure and both Mg and O atoms are exposed at the (001) surface, the adsorbed MgO molecules are stabilized through double coordination even on the smooth MgO(001) surface. This adsorption structure cannot be realized in the deposition process of ZnO molecules on the smooth ZnO(0001) surface, as mentioned before. Consequently, the surface morphology of the metal oxide surfaces is found to have a major influence on the homoepitaxial growth process.

IV. CONCLUSION

The homoepitaxial growth processes of the ZnO(0001) surface are successfully simulated by our crystal-growth MD code. We clarified that the ZnO molecule adsorbed at the surface step has a role of nucleation center and the crystal growth starts from the surface step. The spiral growth mode of the ZnO(0001) surface observed by experiments, is well interpreted from the above crystal-growth mechanism, since a spiral growth is realized by the step flow growth with screw dislocation. The above epitaxial growth mechanism is completely different from that of MgO(001).[30,31] This difference is clearly interpreted from the different surface structures of ZnO(0001) and MgO(001).

Since we modeled the ZnO(0001) surface with a single step in the present paper, the crystal growth process of the ZnO(0001) surface stopped after the first ZnO layer was completed following the step flow mechanism and the step was lost. On the other hand, the screw dislocation observed in the experiments does not lose the step of the ZnO(0001) surface and the crystal-growth process continuously proceeds. Hence, another efficient simulation model is needed to reproduce the step flow mechanism with screw dislocation in future work. However, the present simulations well elucidated the atomistic mechanism of the homoepitaxial growth process of the ZnO(0001) surface and supported the experimental observation.

*Author to whom all correspondence should be addressed.

[1] *Chemical Designing and Processing of High-T_c Superconductors*, edited by M. Kawai and K. Kishio, special issue of Physica C **190** (1991).

[2] *Proceedings of the International Conference on Materials and Mechanisms of Superconductivity High-Temperature Superconductors III*, edited by Tachiki, Y. Muto, and Y. Shono, special issue of Physica C **185-189** (1991).

[3] *Atomically Controlled Surfaces and Interfaces*, edited by M. Tsukada and A. Kawazu, special issue of Appl. Surf. Sci. **60-61** (1992).

[4] *Proceedings of the International Conference on Materials and Mechanisms of Superconductivity High-Temperature Superconductors IV*, edited by P. Wyder, special issue of Physica C **235-240** (1994).

[5] *Crystal Engineering of High-T_c-Related Oxide Films*, edited by H. Koinuma, special issue of MRS Bull. **14** (1994).

[6] *Proceedings of the Second International Symposium of Atomically Controlled Surfaces and Interfaces*, edited by M. Lekela, special issue of Appl. Surf. Sci. **75** (1994).

[7] M. A. Haase, J. Qiu, J. M. Depuydt, and H. Cheng, Appl. Phys. Lett. **59**, 1272 (1991).

[8] S. Taniguchi, T. Hino, S. Itoh, N. Norikazu, A. Ishibashi, and M. Ikeda, Electron. Lett. **32**, 552 (1996).

[9] S. Nakamura, T. Mukai, and M. Senoh, Appl. Phys. Lett. **64**, 1687 (1994).

[10] S. Nakamura, M. Senoh, S. Nagahama, N. Iwasawa, T. Yamada, T. Matsushita, H. Kiyoku, and Y. Sugimoto, Jpn. J. Appl. Phys., Part 2 **35**, L74 (1996).

[11] P. Yu, Z. K. Tang, G. K. L. Wong, M. Kawasaki, A. Ohtomo, H. Koinuma, and Y. Segawa, Proceedings of the 23rd International Conference on the Physics of Semiconductors, 1996 (unpublished), p. 1453.

[12] P. Yu, Z. K. Tang, G. K. L. Wong, M. Kawasaki, A. Ohtomo, H. Koinuma, and Y. Segawa, Solid State Commun. **103**, 459 (1997).

[13] Z. K. Tang, P. Yu, G. K. L. Wong, M. Kawasaki, A. Ohtomo, H. Koinuma, and Y. Segawa, Nonlinear Opt. **18**, 355 (1997).

[14] T. Ohnishi, A. Ohtomo, M. Kawasaki, K. Takahashi, M. Yoshimoto, and H. Koinuma, Appl. Phys. Lett. **72**, 824 (1998).

[15] A. Ohtomo, M. Kawasaki, Y. Sakurai, Y. Yoshida, H. Koinuma, P. Yu, Z. K. Tang, G. K. L. Wong, and Y. Segawa, Mater. Sci. Eng., B **54**, 24 (1998).

[16] P. Yu, Z. K. Tang, G. K. L. Wong, M. Kawasaki, A. Ohtomo, H. Koinuma, and Y. Segawa, J. Cryst. Growth **185**, 601 (1998).

[17] A. Ohtomo, M. Kawasaki, T. Koida, K. Masubuchi, H. Koinuma, Y. Sakurai, Y. Yoshida, T. Yasuda, and Y. Segawa, Appl. Phys. Lett. **72**, 2466 (1998).

[18] D. M. Bagnall, Y. F. Chen, Z. Zhu, T. Yao, S. Koyama, M. Y. Shen, and T. Goto, Appl. Phys. Lett. **70**, 2230 (1997).

[19] Y. Chen, D. M. Bagnall, Z. Zhu, T. Sekiuchi, K. Park, K. Hiraga, and T. Yao, J. Cryst. Growth **181**, 165 (1997).

[20] M. Schneider, I. K. Schuller, and A. Rahman, Phys. Rev. B **36**, 1340 (1987).

[21] E. T. Gawlinski and J. D. Gunton, Phys. Rev. B **36**, 4774 (1987).

[22] R. Biswas, G. S. Grest, and C. M. Soukoulis, Phys. Rev. B **38**, 8154 (1988).

[23] W. D. Luedtke and U. Landman, Phys. Rev. B **40**, 11 733 (1989).

[24] M. F. Crowley, D. Srivastava, and B. J. Garrison, Surf. Sci. **284**, 91 (1993).

[25] W. D. Luedtke and U. Landman, Phys. Rev. B **44**, 5970 (1991).
[26] D. C. Athanasopoulos and S. H. Garofalini, J. Chem. Phys. **97**, 3775 (1992).
[27] M. Kubo, R. Yamauchi, R. Vetrivel, and A. Miyamoto, Appl. Surf. Sci. **82/83**, 559 (1994).
[28] M. Kubo, R. Miura, R. Yamauchi, R. Vetrivel, and A. Miyamoto, Appl. Surf. Sci. **89**, 131 (1995).
[29] M. Kubo, R. Miura, R. Yamauchi, R. Vetrivel, E. Broclawik, and A. Miyamoto, Jpn. J. Appl. Phys., Part 1 **34**, 6873 (1995).
[30] M. Kubo, Y. Oumi, R. Miura, A. Fahmi, A. Stirling, A. Miyamoto, M. Kawasaki, M. Yoshimoto, and H. Koinuma, J. Chem. Phys. **107**, 4416 (1997).
[31] M. Kubo, Y. Oumi, R. Miura, A. Stirling, and A. Miyamoto, AIChE. J. **43**, 2765 (1997).
[32] M. Kubo, Y. Oumi, R. Miura, A. Stirling, A. Miyamoto, M. Kawasaki, M. Yoshimoto, and H. Koinuma, Phys. Rev. B **56**, 13 535 (1997).
[33] M. Kubo, Y. Oumi, R. Miura, A. Stirling, A. Miyamoto, M. Kawasaki, M. Yoshimoto, and H. Koinuma, J. Chem. Phys. **109**, 8601 (1998).
[34] M. Kubo, Y. Oumi, R. Miura, A. Stirling, A. Miyamoto, M. Kawasaki, M. Yoshimoto, and H. Koinuma, J. Chem. Phys. **109**, 9148 (1998).
[35] N. Kumagai, K. Kawamura, and T. Yokokawa, Mol. Simul. **12**, 177 (1994).
[36] M. Kubo, Y. Oumi, H. Takaba, A. Chatterjee, and A. Miyamoto, J. Phys. Chem. B **103**, 1876 (1999).
[37] *Insight II User Guide 4.0.0* (Molecular Simulations Inc., San Diego, 1996).
[38] R. Miura, H. Yamano, R. Yamauchi, M. Katagiri, M. Kubo, R. Vetrivel, and A. Miyamoto, Catal. Today **23**, 409 (1995).
[39] H. Schulz and K. H. Thiemann, Solid State Commun. **32**, 783 (1979).
[40] *Handbook of Physical Quantities*, edited by I. S. Grigoriev and E. Z. Meilikhov (CRC, Boca Raton, 1997).
[41] R. W. G. Wyckoff, *Crystal Structure*, Vol. 1 (Wiley, New York, 1963).
[42] W. L. Bragg and J. A. Darbyshire, Trans. Faraday Soc. **28**, 522 (1932).
[43] J. E. Jaffe and A. C. Hess, Phys. Rev. B **48**, 7903 (1993).
[44] C. B. Duke and Y. R. Wang, J. Vac. Sci. Technol. A **6**, 692 (1988).
[45] J. E. Jaffe, N. M. Harrison, and A. C. Hess, Phys. Rev. B **49**, 11 153 (1994).
[46] P. Schröer, P. Krüger, and J. Pollmann, Phys. Rev. B **49**, 17 092 (1994).
[47] M. Nyberg, M. A. Nygren, L. G. M. Pettersson, D. H. Gay, and A. L. Rohl, J. Phys. Chem. **100**, 9054 (1996).
[48] *Dmol 96.0/4.0.0 User Guide* (Molecular Simulations Inc., San Diego, 1996).
[49] S. H. Vosko, L. Wilk, and M. Nusair, Can. J. Phys. **58**, 1200 (1980).
[50] B. Delley, J. Chem. Phys. **92**, 508 (1990).